34回日本高血圧学会総会 2011年10月22日 栃木県総合文化センター（栃木県 宇都宮市）

12. Koichi Nishiyama, Satoshi Aria, Toshiaki Ko, Yuichiro Arima, Yuji Hakozaki, Kei Sugihara, Hiroaki Koseki, Yasunobu Uchijima, Yukiko Kurihara, Hiroki Kurihara. 「Dynamic and Heterogeneous collective endothelial cell movement driving angiogenic morphogenesis」 The Second Pacific Symposium on Vascular Biology 2011年10月30日 済州新羅ホテル（韓国）

13. Yuichiro Arima, Sachiko Miyagawa-Tomita, Koichi Nishiyama, Rieko Asai, Ki-Sung Kim, Yasunobu Uchijima, Hisao Ogawa, Yukiko Kurihara, Hiroki Kurihara 「Novel roles of the Endothelin-1 and Endothelin A receptor signaling in coronary artery formation.」 日蘭二国間交流セミナー Frontiers Angiogenesis: Development and Diseases 2011年11月5日 昭和薬科大学（東京都 町田市）

14. Koichi Nishiyama, Satoshi Aria, Toshiaki Ko, Yuichiro Arima, Yuji Hakozaki, Kei Sugihara, Hiroaki Koseki, Yasunobu Uchijima, Yukiko Kurihara, Hiroki Kurihara. 「Collective endothelial cell movement in angiogenic morphogenesis」 American Heart Association Scientific Session 2011年11月15日 オーランドコンベンションセンター（米国）

15. Yuichirou Arima, Sachiko Miyagawa-Tomita, Koichi Nishiyama, Rieko Asai , Ki-Sung Kim, Yasunobu Uchijima, Hisao Ogawa, Yukiko Kurihara, Hiroki Kurihara. 「Coronary artery anomalies in Endothelin-1 and Endothelin A receptor knockout mice.」 American Heart Association Scientific Session 2011年11月15日 オーランドコンベンションセンター（米国）

16. Yuichirou Arima, Sachiko Miyagawa-Tomita, Koichi Nishiyama, Rieko Asai , Ki-Sung Kim, Yasunobu Uchijima, Hisao Ogawa, Yukiko Kurihara, Hiroki Kurihara.「Neural crest cells contribute to coronary artery development through endothelin signaling.」第19回日本血管生物医学会学術集会 2011年12月10日 東京ステーションコンファレンス(東京都 千代田区)

17. Ki-Sung Kim, Yuichiro Arima, Rieko Asai, Takahiro Sato, Yasunobu Uchijima, Koichi Nishiyama, Yukiko Kurihara, Takashi Igarashi, Hiroki Kurihara. 「Endothelin-1/Endothelin type-A receptor signaling regulates pharyngeal arch artery development through Dlx5/6-independent pathway.」第19回日本血管生物医学会学術集会 2011年12月10日 東京ステーションコンファランス（東京都 千代田区）

18. 栗原 由紀子, 内島 泰信, 櫛山 櫻, 濱崎 真夏, 西山 功一, 栗原 裕基「下顎形成におけるエンドセリンシグナルにおけるnon-coding RNA とパラスペックル蛋白の作用」 第34回 日本分子生物学会 2011年12月13日 パシフィコ横浜(神奈川県 横浜市)

19. 河村悠美子, 内島泰信, 藤澤興, 西山功一, 浅野知一郎, 栗原由紀子, 栗原裕基「Physiological roles of Sirt3 in mouse preimplantation embryo development (マウス初期胚発生における Sirt3 の機能と生理的役割の解明)」 第34回 日本分子生物大会 2011年12月13日 パシフィコ横浜(神奈川県 横浜市)

20. Taro Kitazawa, Kou Fujisawa, Yukiko Kurihara, Yuichiro Arima, Yumiko Kawamura, Takahiro Sato, Yasunobu Uchijima, Hiroki Kurihara「Hox gene function and possible crosstalk with Dlx genes in craniofacial morphogenesis」 第34回 日本分子生物学会 2011年12月13日 パシフィコ横浜（神奈川県 横浜市）

21. Rieko Asai, Yukiko Kurihara, Yuichirou Arima, Ki-sung Kim, Sachiko Miyagawa-Tomita, Hiroki Kurihara「The first heart field subdomain defined by endothelin receptor type-A expression contributes to conduction system development」第 34 回 日本分子生物学会 2011 年 12 月 13 日 パシフィコ横浜（神奈川県　横浜市）

22. Yuichirou Arima, Sachiko Miyagawa-Tomita, Koichi Nishiyama, Rieko Asai, Ki-Sung Kim, Yasunobu Uchijima, Hisao Ogawa, Yukiko Kurihara, Hiroki Kurihara 「 Endothelin-1/ Endothelin A receptor signaling are required for proper coronary artery development.」第 34 回日本分子生物学会 2011 年 12 月 13 日 パシフィコ横浜（神奈川県　横浜市）

23. Yumiko Kawamura, Yasunobu Uchijima, Kou Fujisawa, Koichi Nishiyama, Yukiko Kurihara and Hiroki Kurihara. 「Protective role of Sirt3 against p53-dependent developmental arrest induced by oxidative stress in preimplantation embryos」 Keystone Symposia “Sirtuins in metabolism, aging and disease” 2012 年 2 月 13 日 Granlibakken Resort (Tahoe City, California, USA)

24. Taro Kitazawa, Kou Fujisawa, Yukiko Kurihara, Yuichiro Arima, Yumiko Kawamura, Takahiro Sato, Yasunobu Uchijima, Hiroki Kurihara「Hox gene function and possible crosstalk with Dlx genes in craniofacial morphogenesis 」 Gordon Research Conference Craniofacial Morphogenesis & Tissue Regeneration 2012 年 3 月 19・20 日 フォーポイント・バイ・シェラトン・ロサンゼルス（米国）

25. Yuichirou Arima, Sachiko Miyagawa-Tomita, Koichi Nishiyama, Rieko Asai , Ki-Sung Kim, Yasunobu Uchijima, Hisao Ogawa, Yukiko Kurihara, Hiroki Kurihara「Novel roles of the neural crest in coronary artery formation through the Endothelin-1/ Endothelin A receptor signaling.」 第 76 回日本循環器学会学術集会 2012 年 3 月 18 日　福岡国際会議場(福岡県　福岡市)

26. Yukiko Kurihara, Yasunobu Uchijima, Sakura Kushiyama, Hiroki Kurihara「Involvement of non-coding RNA: Evf2 in the Endothelin signaling in branchial arch development」 Keystone Symposia Canference Non-Coding RNAs 2012 年 4 月 2 日 スノウバード・クリフロッジ（米国）

H. 知的財産権の出願・登録状況
該当なし

厚生労働科学研究費補助金（創薬基盤推進研究事業）
分担研究報告書

ETAR 発現細胞の解析と血管新生過程の細胞動態に関する研究

研究分担者　西山　功一　東京大学大学院医学系研究科助教

研究要旨
本研究において、本研究において、RMCE により樹立された ETAR-lacZ, ETAR-EGFP マウスを用いて、心血管系における ETAR 発現細胞の動態解析を行った。ETAR 発現心筋細胞が、心形成過程で流入路から上行して心室筋や心房筋に分化する特徴的な細胞系譜を示すこと、血管心血管系における ETAR 発現細胞の系においては平滑筋細胞に広く発現し、特に腎臓においては血管平滑筋細胞、周皮細胞、傍糸球体細胞に強い発現が認められた。これらの発現パターンの解析は、本研究における病態解析の重要な基盤となるとともに、心臓発生のメカニズムを理解する上でも重要な知見となった。さらに、血管新生過程の細胞動態の可視化とコンピューター解析により樹状構造を形成する細胞の複雑な振る舞いや先端細胞の入れ替わり現象を明らかにし、血管新生機構の新しい理解に貢献した。

A．研究目的

RMCE により樹立された ETAR-lacZ, ETAR-EGFP マウスを用いて心血管系における ETAR 発現動態を解析し、ETAR 発現細胞の発生学的役割を明らかにするとともに、病態モデルマウス作成に基盤となる情報を提供する。さらに、血管新生過程の細胞動態の可視化とコンピューター解析により、樹状構造形成における細胞動態と細胞間相互作用機構を明らかにする。

B．研究方法

1．遺伝子改変マウス

ETAR-lacZ, ETAR-EGFP マウスは、既報の通りリコンビナーゼ依存性カセット交換（RMCE）を用いて作成した。即ち、ETAR 遺伝子第２エクソンに変異型 lox 配列（lox71, lox2272）で挟んだ neomycin 耐性遺伝子を導入した ES 細胞に対し、上記変異型 lox に対応する配列（lox66, lox2272）で挟んだ lacZ, EGFP 遺伝子断片それぞれを含むプラスミドを電気穿孔法で導入して Cre リコンビナーゼ遺伝子を含むアデノウィルスベクター（AxCANCre）を感染させて lox 配列に相同組み換えを起こさせ、導入遺伝子を ETAR 遺伝子座にノックインした ES 細胞株を得た。これらよりキメラマウスを作成し、生殖細胞系列に寄与したキメラマウスよりノックインマウスを得た。

マウスは温度 23±2°C、湿度 50-60%、12 時間毎の明暗サイクル下に飼育し、実験に供した。実験は東京大学動物実験規則に則り、東京大学医学系研究科動物実験委員会により承認された実験計画のもとで行われた。

2．β-ガラクトシダーゼ染色

LacZ 遺伝子発現によるβ-ガラクトシダーゼの酵素活性は、全胚固定標本または凍結切片標本において、X-gal (5-bromo-4-chloro-3-indoyl β-D-galactoside) を基質とした発色反応により検出した。

3．免疫染色

凍結切片標本において、一次抗体反応後にペルオキシダーゼ、FITC、ビオチンで標識した二次抗体を反応させ、蛍光または発色反応によって可視化した。

4．大動脈リングアッセイ

マウスより摘出し、周囲の脂肪・結合織を取り除いた大動脈の組織小片を I 型コラーゲンゲル上に静置し、medium-199＋5%胎仔ウシ血清＋50 ng/ml ヒト型リコンビナント VEGF 存在下で培養した。

5．マウス生体内での網膜血管新生解析

蛍光ラベルした BS-1 レクチンを生後１日のマウス心腔内に注射し、網膜新生血管への取り込

みを経時的に追跡した。

６．タイムラプスイメージング

大動脈リングアッセイ開始５～６日後、蛍光色素 SYTO-16 または SYTO-61 (0.1 μg/ml, Molecular Probes)で内皮細胞をラベルし（内皮細胞が選択的ラベルされることは、細胞カーカーとの二重染色、FACS 解析により証明)、タイムラプス画像を共焦点レーザー走査型顕微鏡（オリンパス FluoView FV10i）により 15 分毎に 36 時間にわたって記録した。得られた画像を、FLUOVIEW ソフトウェアを用いてデジタル化し、解析に供した。

細胞のモザイク解析では、培養開始前に EGFP 発現アデノウィルスを大動脈リング標本に感染させた。ウィルス力価は、一部の内皮細胞が感染するように条件を設定した。

７．コンピューター解析

ImageJ、MTrackJ、MATLAB の解析ソフトを用いて、以下の解析を行った。ラベルされた各細胞をマニュアルでプロットし、その時系列データをピクセル座標として蓄積した。各分枝の伸長方向を軸として各プロットの位置と速度を変換した。そのデータから、細胞の速度、方向性の相関、連続性、先端細胞の伸長動態などをモジュール化し、それぞれを表現するパラメータを独立性の検証を経て数値化し、数理統計手法を用いて解析した。

Ｃ．研究結果

１．心血管系における ETAR 発現細胞の解析

ETAR-lacZ または ETAR-EGFP ノックインマウスを用いて、本研究の標的細胞である ETAR 発現心筋細胞の分布と動態を解析した。ETAR-lacZ/EGFP 発現細胞は、マウス E8.0 日胚の心臓原基腹側において最初に認められ、原始心筒形成期には心臓流入路の腹側に局在していた。その発現は、in situ ハイブリダイゼーションによる ETAR 遺伝子の発現パターンとほぼ一致しており、内在性 ETAR の発現を反映すると考えられた。この初期の発現は、一次心臓予定領域マーカーである Nkx2.5・Mlc2a の発現領域の一部と一致していたが、二次心臓予定領域マーカーである Isl1 とは重ならず、ETAR-lacZ/EGFP 発現細胞は一次心臓予定領域に含まれる細胞集団であると考えられた。心ループ形成期には、ETAR-lacZ/EGFP 発現細胞は左側壁から左心室領域にかけて大彎に沿って分布し、四腔形成期にはその発現は左心室と両心房、さらに右心室の一部に広がった。これらの結果とマーカー遺伝子発現の経時的解析から、心臓形成初期における ETAR-lacZ/EGFP 発現細胞は、流入路に生じて原始心筒～心ループ形成期に上方へ移動する細胞群と考えられた。

血管系においては、大動脈や脳血管など広く血管平滑筋において ETAR-lacZ の発現が認められた。特に、腎臓では腎形成初期より未分化間葉細胞に発現し、その後血管平滑筋細胞、周皮細胞、レニン分泌細胞である傍糸球体細胞に強い発現が認められた。

２．血管新生における細胞動態の解析

成獣 ETAR-EGFP マウスより大動脈組織片を摘出し、I 型コラーゲンゲル上で組織培養を行い、出芽による血管新生様の樹枝状構造伸長過程を観察した。CD31 による血管内皮細胞の同定、他の平滑筋マーカーとの共染色から、EGFP は血管平滑筋細胞に選択的に発現することが示された。この過程を血管新生モデルとして血管内皮細胞を選択的に SYTO 蛍光色素でラベルし、タイムラプスイメージングを行うことにより、従来予想されていた以上に細胞が複雑な動態を示すことが明らかになった。特に、内皮細胞は全体としての樹枝状構造を保持しながら常に異なる速度で遊走し、相互の相対的位置関係を常に変えていく混合現象を呈した。また、これまで特定の形質をもつ細胞と考えられていた先端細胞（tip cell）は恒常的なものではなく、細胞の追い越し現象によって常に入れ替わっていくことが明らかになった。こうした現象は、マウス生体内での網膜血管新生過程で起きていることも、レクチンを用いた内皮細胞ラベリングで明らかになった。

さらに、新たに示された細胞動態の生理的意義や分子機序を明らかにするため、得られたタイムラプス画像から細胞一つ一つの位置情報を時間軸に沿って抽出し、それを基に細胞動態を特徴づけるパラメータを設定し定量評価した。血管新生は、血管の伸長や分岐といった質的に異なる要素（モジュール）が時空間的に組み合わさることにより血管全体の形態的構造が構築されていると考えることができる。そこで、モジュールの一つである血管伸長の検討を行った。最も代表的な血管新生促進因子である VEGF の作用点に関して検討した結果、VEGF は血管内皮細胞の平均速度の増加や方向性運動の質的向上、さらに先端細胞の遊走距離増加を介して、血管

伸長に対して促進的に作用することが示唆された。さらに薬理学的実験から、VEGF によって誘導される血管伸長反応の一部は、Delta-like 4-Notch シグナルを介した内皮細胞間相互作用により負に制御されること、また内皮細胞と EGFP でラベルされる平滑筋細胞間の相互作用により正に制御されていることが示され、早期血管新生における内皮細胞−平滑筋細胞間相互作用の役割が示唆された。

D．考察

心臓における ETAR 発現細胞は、主に心流出路〜大血管起始部に寄与する心臓神経堤細胞と、心室心房領域の作業心筋の２つに大別されるが、本研究では後者に関し、心臓形成の初期からその起源となる領域と動態を lacZ/EGFP ノックインマウスを用いて明らかにした。加えて、血管系、特に腎臓における ETAR の発現動態を明らかにし、腎疾患や高血圧などの病態理解に重要な知見となった。

血管新生過程の細胞動態の解析は、血管新生における樹状構造形成の細胞生物学的基盤に新しい理解を与えるものであり、血管系の病態研究にも意義の大きい知見と考えられた。

E．結論

本研究において、心血管系における ETAR 発現細胞の動態を明らかにし、本研究における病態解析の重要な基盤を提供した。さらに、血管新生過程の細胞動態の可視化とコンピューター解析により樹状構造を形成する細胞の複雑な振る舞いや先端細胞の入れ替わり現象を明らかにし、血管新生機構の新しい理解に貢献した。

F．健康危険情報

該当なし

G．研究発表

1. 論文発表

1. Arima S, Nishiyama K, Ko T, Arima Y, Hakozaki Y, Sugihara K, Koseki H, Uchijima Y, Kurihara Y, Kurihara H. (2011). Angiogenic morphogenesis driven by dynamic and heterogeneous collective endothelial cell movement. *Development* 138, 4763-4776.

2. Kitazawa T, Sato T, Nishiyama K, Asai R, Arima Y, Uchijima Y, Kurihara Y, Kurihara H. (2011). Identification and developmental analysis of endothelin receptor type-A expressing cells in the mouse kidney. *Gene Expr. Patterns.* 11, 371-377.

3. Tonami K, Kurihara Y, Arima S, Nishiyama K, Uchijima Y, Asano T, Sorimachi H, Kurihara H. (2011). Calpain 6, a microtubule-stabilizing protein, regulates Rac1 activity and cell motility through interaction with GEF-H1. *J. Cell Sci.* 124, 1214-1223.

2. 学会発表

1. Ki-Sung Kim, Yuichiro Arima, Rieko Asai, Takahiro Sato, Yasunobu Uchijima, Koichi Nishiyama, Yukiko Kurihara, Takashi Igarashi, Hiroki Kurihara. 「Endothelin-1/Endothelin type-A receptor signaling regulates pharyngeal arch artery development through Dlx5/6-independent pathway.」 2011 Pediatric Academic Societies and Asian Society for Pediatric Research joint meeting 2011 年 5 月 1 日 Denver Convention Center, (Denver, USA)

2. Koichi Nishiyama 「Collective endothelial cell movement in angiogenic morphogenesis」 The 9th Japan-Korea Joint Symposium on vascular biology（招待講演）2011 年 8 月 25 日 ウエスティン朝鮮ホテル釜山(韓国)

3. Koichi Nishiyama, Satoshi Aria, Toshiaki Ko, Yuichiro Arima, Yuji Hakozaki, Kei Sugihara, Hiroaki Koseki, Yasunobu Uchijima, Yukiko Kurihara, Hiroki Kurihara. 「Id1 modulates sprouting angiogenesis possibly via spatiotemporal regulation of the Notch signal specification」 第 84 回 日本生化学大会 2011 年 9 月 22 日 国立京都国際会館 (京都府 京都市)

4. 河村 悠美子, 内島泰信, 藤澤興, 西山功一, 栗原由紀子, 栗原裕基.「Sirt3 による酸化

ストレス防御機構の初期胚発生における役割」第84回 日本生化学会大会 2011年9月24日 国立京都国際会館（京都府 京都市）

5. 金基成，有馬勇一郎，淺井理恵子，佐藤崇博，内島泰信，西山功一，五十嵐隆，栗原由紀子，栗原裕基.「エンドセリンシグナルによる咽頭弓動脈リモデリング機構の解明」第10回心臓血管発生研究会 2011年10月7日 ホテル華の湯（福島県 郡山市）

6. 有馬勇一郎，宮川-富田幸子，西山功一，淺井理恵子，金基成，小川久雄，栗原由紀子，栗原裕基.「冠動脈形成における神経堤細胞の新しい役割 -マウスからみた神経堤細胞と冠動脈形成-」第10回心臓血管発生研究会 2011年10月7日 ホテル華の湯（福島県 郡山市）

7. 淺井理恵子，栗原由紀子，有馬勇一郎，金基成，西山功一，内島泰信，中野敦，宮川-富田幸子，栗原裕基.「In vitro/in vivo刺激伝導系形成モデル確立の試み.」第10回心臓血管発生研究会2011年10月8日 ホテル華の湯（福島県 郡山市）

8. 西山功一，有馬聡，有馬勇一郎，金基成，内島泰信，栗原由紀子，栗原裕基.「Ex vivoにおける定量的血管新生評価系の開発」第34回日本高血圧学会総会 2011年10月22日 栃木県総合文化センター（栃木県 宇都宮市）

9. Koichi Nishiyama, Satoshi Aria, Toshiaki Ko, Yuichiro Arima, Yuji Hakozaki, Kei Sugihara, Hiroaki Koseki, Yasunobu Uchijima, Yukiko Kurihara, Hiroki Kurihara. 「Dynamic and Heterogeneous collective endothelial cell movement driving angiogenic morphogenesis」 The Second Pacific Symposium on Vascular Biology 2011年10月30日 済州新羅ホテル（韓国）

10. Koichi Nishiyama, Satoshi Aria, Hiroki Kurihara.「Morphogenetic cell movement in sprouting angiogenesis」 日蘭二国間交流セミナーFrontiers Angiogenesis: Development and Diseases(招待講演)2011年11月4日 昭和薬科大学（東京都 町田市）

11. Yuichiro Arima, Sachiko Miyagawa-Tomita, Koichi Nishiyama, Rieko Asai, Ki-Sung Kim, Yasunobu Uchijima, Hisao Ogawa, Yukiko Kurihara, Hiroki Kurihara 「Novel roles of the Endothelin-1 and Endothelin A receptor signaling in coronary artery formation.」 日蘭二国間交流セミナーFrontiers Angiogenesis: Development and Diseases 2011年11月5日 昭和薬科大学（東京都 町田市）

12. Koichi Nishiyama, Satoshi Aria, Toshiaki Ko, Yuichiro Arima, Yuji Hakozaki, Kei Sugihara, Hiroaki Koseki, Yasunobu Uchijima, Yukiko Kurihara, Hiroki Kurihara. 「Collective endothelial cell movement in angiogenic morphogenesis」 American Heart Association Scientific Session 2011年11月15日 オーランドコンベンションセンター（米国）

13. Yuichirou Arima, Sachiko Miyagawa-Tomita, Koichi Nishiyama, Rieko Asai , Ki-Sung Kim, Yasunobu Uchijima, Hisao Ogawa, Yukiko Kurihara, Hiroki Kurihara. 「Coronary artery anomalies in Endothelin-1 and Endothelin A receptor knockout mice.」 American Heart Association Scientific Session 2011年11月15日 オーランドコンベンションセンター（米国）

14. Koichi Nishiyama, Hiroki kurihara. 「Mechanism involving dynamic and heterogeneous endothelial cell movement during angiogenesis」 第19回日本血管生物医学会学術集会(招待講演) 2011年12月9日 東京ステーションコンファレンス（東京都 千代田区）

15. Yuichirou Arima, Sachiko Miyagawa-Tomita, Koichi Nishiyama, Rieko Asai , Ki-Sung Kim, Yasunobu

Uchijima, Hisao Ogawa, Yukiko Kurihara, Hiroki Kurihara.「Neural crest cells contribute to coronary artery development through endothelin signaling.」第 19 回日本血管生物医学会学術集会 2011 年 12 月 10 日 東京ステーションコンファレンス(東京都 千代田区)

16. Ki-Sung Kim, Yuichiro Arima, Rieko Asai, Takahiro Sato, Yasunobu Uchijima, Koichi Nishiyama, Yukiko Kurihara, Takashi Igarashi, Hiroki Kurihara.「Endothelin-1/Endothelin type-A receptor signaling regulates pharyngeal arch artery development through Dlx5/6-independent pathway.」第 19 回日本血管生物医学会学術集会 2011 年 12 月 10 日 東京ステーションコンファランス(東京都 千代田区)

17. Koichi Nishiyama, Satoshi Arima, Hiroki Kurihara「Angiogenic morphogenesis driven by collective endothelial cell behavior」第 34 回分子生物学会年会(招待講演) 2011 年 12 月 13 日 パシフィコ横浜(神奈川県 横浜市)

18. 栗原 由紀子, 内島 泰信, 櫛山 櫻, 濱崎 真夏, 西山 功一, 栗原 裕基「下顎形成におけるエンドセリンシグナルにおける non-coding RNA とパラスペックル蛋白の作用」 第 34 回 日本分子生物学会 2011 年 12 月 13 日 パシフィコ横浜(神奈川県 横浜市)

19. 河村悠美子, 内島泰信, 藤澤興, 西山功一, 浅野知一郎, 栗原由紀子, 栗原裕基「Physiological roles of Sirt3 in mouse preimplantation embryo development (マウス初期胚発生における Sirt3 の機能と生理的役割の解明)」 第 34 回 日本分子生物大会 2011 年 12 月 13 日 パシフィコ横浜(神奈川県 横浜市)

20. Yuichirou Arima, Sachiko Miyagawa-Tomita, Koichi Nishiyama, Rieko Asai, Ki-Sung Kim, Yasunobu Uchijima, Hisao Ogawa, Yukiko Kurihara, Hiroki Kurihara「Endothelin-1/Endothelin A receptor signaling are required for proper coronary artery development.」第 34 回日本分子生物学会 2011 年 12 月 13 日 パシフィコ横浜(神奈川県 横浜市)

21. 牧野智行, 宮川-富田幸子, 立花誠, 眞貝洋一, 竹内隆. 「ヒストンメチラーゼ G9a および GLP の心筋細胞特異的欠損マウスにおける心臓形態形成異常の解析.」第 34 回日本分子生物学会 2011 年 12 月 13 日 パシフィコ横浜(神奈川県 横浜市)

22. Yumiko Kawamura, Yasunobu Uchijima, Kou Fujisawa, Koichi Nishiyama, Yukiko Kurihara and Hiroki Kurihara.「Protective role of Sirt3 against p53-dependent developmental arrest induced by oxidative stress in preimplantation embryos」 Keystone Symposia "Sirtuins in metabolism, aging and disease" 2012 年 2 月 13 日 Granlibakken Resort (Tahoe City, California, USA)

23. 西山功一, 栗原裕基「Ex vivo 血管新生における血管内皮細胞の集団的運動」第 117 回日本解剖学会総会・全国学術集会(招待講演) 2012 年 3 月 26 日 山梨大学(山梨県 甲府市)

24. Yuichirou Arima, Sachiko Miyagawa-Tomita, Koichi Nishiyama, Rieko Asai , Ki-Sung Kim, Yasunobu Uchijima, Hisao Ogawa, Yukiko Kurihara, Hiroki Kurihara「Novel roles of the neural crest in coronary artery formation through the Endothelin-1/Endothelin A receptor signaling.」第 76 回日本循環器学会学術集会 2012 年 3 月 18 日 福岡国際会議場(福岡県 福岡市)

H. 知的財産権の出願・登録状況

該当なし

厚生労働科学研究費補助金（創薬基盤推進研究事業）
分担研究報告書

心血管系の細胞系譜に関する研究

研究分担者　富田　幸子　東京女子医科大学医学部助教

研究要旨
ETAR-lacZ, ETAR-EGFP マウスより明らかにされた ETAR 発現心筋細胞の動態を解析し、心発生初期において、エンドセリン-A 受容体発現細胞群が一次心臓領域の腹側に特異的な心臓起源領域を形成すること、原始心筒形成後に心流入路から左側壁を上行して左室と両心房の心筋に分化することを明らかにした。さらに、マウス-ニワトリのキメラ作成系を確立し、心流入路の細胞群が左室心筋に寄与することを明らかにした。これらの実験系と得られた知見は、心血管系の疾患モデルマウスの表現型解析に有用なアプローチ法と視点を提供すると考えられる。

Ａ．研究目的

循環器疾患の発生学的理解は、これまで先天性心疾患に限られていたが、最近は成人以降に発症する疾患においても、その発症原因となる細胞の発生学的系譜や発生過程での異常の観点から理解することの重要性が指摘され始めている。本研究では、RMCE により作成された ETAR-lacZ, ETAR-EGFP マウスの解析と鳥類胚を用いた新しい研究手法を通して、マウス発生工学を中心とする本プロジェクトに新しいアプローチ法と視点を提供することを試みた。

Ｂ．研究方法

１．遺伝子改変マウスと鶏卵

Ednra-lacZ, Ednra-EGFP マウスは東京女子医科大学動物実験施設で適正な環境下で飼育し、鶏卵は孵卵器で維持した。実験は東京女子医科大学動物実験規則に則り、同動物実験委員会により承認された実験計画のもとで行われた。

２．β-ガラクトシダーゼ染色

LacZ 遺伝子発現による β-ガラクトシダーゼの酵素活性は、全胚固定標本または凍結切片標本において、X-gal (5-bromo-4-chloro-3-indoyl β-D-galactoside)を基質とした発色反応により検出した。

３．免疫染色

凍結切片標本において、一次抗体反応後にペルオキシダーゼ、FITC、ビオチンで標識した二次抗体を反応させ、蛍光または発色反応によって可視化した。

４．in situ ハイブリダイゼーション

全胚固定標本または凍結切片標本において、digoxigenin で標識した RNA プローブを用いて通常の方法で行った。

５．蛍光色素ラベリング

マウス胎生 8.25 日胚の心流入路領域に対して、蛍光色素 PKH67（緑）または PKH26（赤）をマイクロインジェクションした。その後、DMEM/F2＋50%ラット血清存在下で回転培養を 30 時間行い、蛍光実体顕微鏡（Leica MZFLIII stereomicroscope＋Hamamatsu digital camera C4742-95）で観察した。

６．組織移植・培養

マウス胎生 8.25 日胚の心流入路 EGFP 発現領域より組織片を切り出し、一部の実験では蛍光色素 SYTO16 で細胞をラベルした後、同じ発生段階のマウス胚の流入路領域に移植した。対照群として、心流出路、心筒領域、尾部の組織を移植片に用いた。移植を受けた胚は、α-MEM＋10%ウマ血清存在下で 低酸素状態（5% CO_2、95% N_2）で 24 時間培養し、(5)と同様に観察した。

心筋培養については、マウス胎生 8.25 日胚の心流入路 EGFP 発現領域より組織片を切り出し、トリプシン処理により細胞を単離した後、マウス胎仔心臓より調整した心臓線維芽細胞をフィーダーとして培養した。

７．ニワトリ初期胚操作

ニワトリ初期 2 日胚の心流入路に、胎生 8.25 日（5-7 体節）の lacZ 発現マウスから摘出した心流入路の組織を同所性に in ovo で移植し、3 日後の心臓形成が進んだ後にマウス細胞の寄与を観察した。

Ｃ．研究結果

心臓形成過程における Ednra 発現細胞群の動

態をETAR-lacZおよびETAR-EGFPマウスにより解析した。Ednra 陽性細胞群はマウス胎生 8.0 日胚（E8.0）の心臓原基腹側において最初に認められ、原始心筒形成期には心臓流入路の腹側に局在していた。その後E8.5の心ループ形成期の分布パターンから、Ednra-lacZ陽性細胞群はE8.25の心流入路腹側から左側壁（大彎側）を経て左心室・右心房へ移動する可能性が考えられ、以下の実験により検証した。まず、E8.25 のEdnra 陽性心流入路領域に蛍光色素をマイクロインジェクションし、胎外培養を行った結果、標識された細胞群が左心室及び右心房に向かって移動する様子が観察された。さらに、E8.25 Ednra-EGFP陽性領域を野生型胚心流入路に移植した結果、移植先の左心室でEGFPシグナルが認められた。これらの移動は、心筒中央部（心室）領域、心流出路領域の移植では観察されなかった。同様のキメラ実験を、マウス-ニワトリ胚でも試みた。その結果、ニワトリ胚に移植したマウス心流入路組織は生着して左室内へと取り込まれ、心筋細胞に分化することが細胞特異的マーカーを用いて証明された。

D．考察

Ednra陽性細胞は一次心臓領域の亜集団であり、心ループ形成期に心流入路から大彎を経て左心室や心房に移動し、作業心筋の形成に寄与することが示された。大彎に沿った特徴的分布パターンと細胞移動は、心室筋・心房筋の起源となる細胞の新しい動態を示すとともに、流入路における細胞の出現と上行する細胞移動の方向は、発生初期の刺激伝導系の形成と興奮伝播様式と一致しており、刺激伝導路形成への寄与も考えられる。実際、ETARの最も初期の発現パターンはペースメーカー細胞の特徴である K_f チャネルをコードするHCN4遺伝子の発現パターンとよく一致しており、現在その関連について解析を進めている。また、鳥類胚で改良された技術のマウスへの応用や異種間キメラ胚の作成は、大きさの問題などで困難さは伴うものの、細胞系譜や病態形成に関わる発生基盤の理解に重要なアプローチ法を提供すると考えられる。

E．結論

ETAR発現細胞の心臓発生への寄与に関する新しい知見と発生学的解析法は、心血管系におけるmiRNA特異的発現による疾患モデルの確立と解析に有用と考えられる。

G．研究発表

1．論文発表

1. Ando K, Takahashi M, Yamagishi T, Miyagawa-Tomita S, Imanaka-Yoshida K, Yoshida T, Nakajima Y. (2011) Tenascin C may regulate the recruitment of smooth muscle cells during coronary artery development. Differentiation 81:299-306

2. Obayashi K, *Miyagawa-Tomita S, Matsumoto H, Koyama H, Nakanishi T, Hirose H. (2011) Effects of transforming growth factor-β3 and matrix metalloproteinase-3 on the pathogenesis of chronic mitral valvular disease in dogs. Am J Vet Res 72:194-202.

3. Kudo Y, Kaneko M, Nakazawa M, Miyagawa-Tomita S. (2011) A case of Cor Triatriatum with an abnormal P wave: The pacemaker action from the specialized tissue in the abnormal septum. Pediatric Cardiology 32:1244-148.

2.学会発表

1. Kokubo H, Miyagawa-Tomita S, Nakashima Y, Nakanishi T, Saga Y. 「Hesr2 disrupted mice develop aortic valve disease with advancing age.」Weinstein Cardiovascular Development Conference, 8-17, 2011, May/5-7, Cincinnati, Ohio, USA

2. Asai R, Kurihara Y, Fujisawa K, Sato T, Kawamura Y, Miyagawa-Tomita S, Kurihara H.「Endothelin receptor type-A expression defines a distinct subdomain, within the heart field and contributes to chamber myocardium.」Weinstein Cardiovascular Development Conference, S5-5, 2011, May/5-7, Cincinnati, Ohio, USA

3. Imanaka Y, Ando K, Takahashi M, Yamagishi T, Yoshida T, Nakajima Y,

Miyagawa-Tomita S. 「Matricellular protein, tenascin-C, may regulate proepi/epicardial cell function during coronary vessel development. 」 Weinstein Cardiovascular Development Conference, 6-11, 2011, May/5-7, Cincinnati, Ohio, USA

4. Asai R, Kurihara Y, Fujisawa K, Sato T, Kawamura Y, Kokubo H, Tonami K, Nishiyama K, Uchijima Y, Miyagawa-Tomita S, Kurihara H. 「Endothelin receptor type-A expression defines a distinct subpopulation within the heart field and contributes to chamber myocardium formation. 」 44th Annual Meeting of the Japanese Society of Developmental Biologists, P-2100, 2011, May/18-21, Okinawa

5. 有馬勇一郎、宮川-富田幸子、西山功一、淺井理恵子、金　基成、小川久夫、栗原由紀子、栗原裕基. 「冠動脈形成における神経堤細胞の新しい役割-マウスからみた神経堤細胞と冠動脈形成-.」第 10 回心臓血管発生研究会、6-1、2011 年 10 月 7-8 日、郡山、福島

6. 宮川-富田幸子、有馬勇一郎、前田和宏、栗原裕基. 「冠動脈形成における神経堤細胞の新しい役割-鳥類からみた神経堤細胞と冠動脈形成-.」第 10 回心臓血管発生研究会、6-2、2011 年 10 月 7-8 日、郡山、福島

7. 淺井理恵子、栗原由紀子、有馬勇一郎、金基成、西山功一、内島泰信、中野　敦、宮川-富田幸子、栗原裕基.「in vitro/in vivo 刺激伝導系形成モデル確立の試み. 」第 10 回心臓血管発生研究会、12、2011 年 10 月 7-8 日、郡山、福島

8. Arima Y, Miyagawa-Tomita S, Nishiyama K, Asai R, Kim KS, Uchijima Y, Ogawa H, Kurihara Y, Kurihara H. 「Novel roles of the Endothelin-1 and Endothelin A receptor signaling in coronary artery formation. 」 日蘭二国間交流セミナー Frontiers Angiogenesis: Development and Diseases, 2011 年 11 月 4-6 日、昭和薬科大学

9. Arima Y, Miyagawa-Tomita S, Nishiyama K, Asai R, Kim KS, Uchijima Y, Ogawa H, Kurihara Y, Kurihara H. 「Neural crest cells contribute to coronary artery development through endothelin signaling. 」第 19 回日本血管生物医学界学術集会、2011 年 11 月 8-10 日、東京ステーションコンファレンス、東京

10. Arima Y, Miyagawa-Tomita S, Nishiyama K, Asai R, Kim KS, Uchijima Y, Ogawa H, Kurihara Y, Kurihara H. 「Coronary artery anomalies in Endothelin-1 and Endothelin A receptor knockout mice. 」 Scientific Sessions of the American Heart Association, 2011, Nov/8-10, Orlando, Florida, USA

11. 牧野智行、宮川-富田幸子、立花 誠、眞貝洋一、竹内 隆. 「ヒストンメチラーゼ G9a および GLP の心筋細胞特異的欠損マウスにおける心臓形態形成異常の解析. 」第 34 回日本分子生物学会、1P-0103、横浜

12. Arima Y, Miyagawa-Tomita S, Nishiyama K, Asai R, Kim KS, Uchijima Y, Ogawa H, Kurihara Y, Kurihara H. 「Endothelin-1/Endothelin A receptor signaling are required for proper coronary artery development. 」 The 34th Annual Meeting of the Molecular Biology Society of Japan, 1P-0116, 2011, Dec/13-16, Yokohama

13. Asai R, Kurihara Y, Arima Y, Kim KS, Miyagawa-Tomita S, Kurihara H (2011, Dec 13-16) 「The first heart field subdomain defined by endothelin receptor type-A expression contributes to conduction system development. 」 The 34th Annual Meeting of the Molecular Biology Society of Japan, Working symposium, 1P-0291(1T9pII-5), 2011, Dec/13-16, Yokohama,

14. Miyagawa-Tomita S, Arima S, Kurihara H.

「Novel roles of the neural crest in coronary artery formation through endothelin signaling.」 The 34th Annual Meeting of the Molecular Biology Society of Japan, Working symposium, 1W3pII-4, 2011, Dec/13-16, Yokohama

セミナー

1. 宮川-富田幸子. ファロー四徴症の発生学。第21回東京女子医科大学循環器小児科夏季セミナー、東京

2. 宮川-富田幸子. 冠動脈発育の最近の話題。第51回総合研究所セミナー、東京女子医科大学、東京

翻訳

2. 分担翻訳 “Clinical Veterinary Advisor -Dogs and Cats. Mosby” (Elsevier) 「クリニカルベテリナリーアドバイザー -犬と猫の診療指針-」 総監修 Etienne Cote(2007) Mosby Elsevier Inc., 監訳長谷川篤彦、2010年、interzoo 発行、1851pages

図書

1. 竹内 純、宮川-富田幸子、笹岡陽介、小柴和子。「心臓発生と心筋分化誘導のマスター因子。」 pp.1-16、Annual Review 循環器2011、山口 徹他編集, 中外医学社（総ページ365）

紀要

1. 宮川-富田幸子、中西敏雄、今中-吉田恭子. 心臓血管の発生・発達に関与する遺伝子群の検討. -冠動脈形成におけるテネイシンCの役割-. 東京女子医科大学総合研究所起用2010年度報告書、31、136-137.

H. 知的財産権の出願・登録状況

該当なし

別添５

研究成果の刊行に関する一覧表

別紙４

研究成果の刊行に関する一覧表

雑誌

発表者氏名	論文タイトル名	発表誌名	巻号	ページ	出版年
Arima S*, Nishiyama K*, Ko T, Arima Y, Hakozaki Y, Sugihara K, Koseki H, Uchijima Y, Kurihara Y, Kurihara H. *These authors contributed equally to this work.	Angiogenic morphogenesis driven by dynamic and heterogeneous collective endothelial cell movement.	*Development.*	138	4763-4776	2011
Kitazawa T, Sato T, Nishiyama K, Asai R, Arima Y, Uchijima Y, Kurihara Y, Kurihara H.	Identification and developmental analysis of endothelin receptor type-A expressing cells in the mouse kidney.	*Gene Expr. Patterns.*	11	371-377	2011
Tonami K, Kurihara Y, Arima S, Nishiyama K, Uchijima Y, Asano T, Sorimachi H, Kurihara H.	Calpain 6, a microtubule-stabilizing protein, regulates Rac1 activity and cell motility through interaction with GEF-H1.	*J. Cell Sci.*	124	1214-1223	2011
Ando K, Takahashi M, Yamagishi T, Miyagawa-Tomita S, Imanaka-yoshida K, Yoshida T, Nakajima Y.	Immunolocalization of tenascin C during proximal coronary arteriogenesis:possible role in mural development.	*Differentiation*	81	299-306	2011
Obayashi K, Miyagawa-Tomita S, Matsumoto H, Koyama H, Nakanishi T, Hirose H.	Effects of transforming growth factor-β3 and matrix metalloproteinase-3 on the pathogenesis of chronic mitral valvular disease in dogs.	*Am J Vet Res*	72	194-202	2011
Kudo Y, Kaneko M, Nakazawa M, Tomita S.	A case of Cor Triatriatum with an abnormal P wave: The pacemaker action from the specialized tissue in the abnormal septum.	*Pediatric Cardiology*	32	1244-1248	2011
Kushiyama A, Okubo H, Sakoda H, Kikuchi T, Fujishiro M, Sato H, Kushiyama S, Iwashita M, Nishimura F, Fukushima T, Nakatsu Y, Kamata H, Kawazu S, Higashi Y, Kurihara H, Asano T.	Xanthine Oxidoreductase Is Involved in Macrophage Foam Cell Formation and atherosclerosis development.	*Arterioscler Thromb Vasc Biol.*	32	291-298	2012

Development 138, 4763-4776 (2011) doi:10.1242/dev.068023
© 2011. Published by The Company of Biologists Ltd

Angiogenic morphogenesis driven by dynamic and heterogeneous collective endothelial cell movement

Satoshi Arima*, Koichi Nishiyama*,†, Toshiyuki Ko, Yuichiro Arima, Yuji Hakozaki, Kei Sugihara, Hiroaki Koseki, Yasunobu Uchijima, Yukiko Kurihara and Hiroki Kurihara

SUMMARY

Angiogenesis is a complex process, which is accomplished by reiteration of modules such as sprouting, elongation and bifurcation, that configures branching vascular networks. However, details of the individual and collective behaviors of vascular endothelial cells (ECs) during angiogenic morphogenesis remain largely unknown. Herein, we established a time-lapse imaging and computer-assisted analysis system that quantitatively characterizes behaviors in sprouting angiogenesis. Surprisingly, ECs moved backwards and forwards, overtaking each other even at the tip, showing an unknown mode of collective cell movement with dynamic 'cell-mixing'. Mosaic analysis, which enabled us to monitor the behavior of individual cells in a multicellular structure, confirmed the 'cell-mixing' phenomenon of ECs that occurs at the whole-cell level. Furthermore, an in vivo EC-tracking analysis revealed evidence of cell-mixing and overtaking at the tip in developing murine retinal vessels. In parametrical analysis, VEGF enhanced tip cell behavior and directed EC migration at the stalk during branch elongation. These movements were counter-regulated by EC-EC interplay via γ-secretase-dependent Dll4-Notch signaling, and might be promoted by EC-mural cell interplay. Finally, multiple regression analysis showed that these molecule-mediated tip cell behaviors and directed EC migration contributed to effective branch elongation. Taken together, our findings provide new insights into the individual and collective EC movements driving angiogenic morphogenesis. The methodology used for this analysis might serve to bridge the gap in our understanding between individual cell behavior and branching morphogenesis.

KEY WORDS: Angiogenesis, Time-lapse imaging, Collective cell movement, Mouse

INTRODUCTION

Morphogenetic cell movement gives rise to various types of geometry observed in the living world. The processes are diverse, and recently the notion of collective cell movement has increasingly become a focus of research. Known collective cell movements include branching morphogenesis of the mammary gland, cluster movement of detached cancer cells, border cell migration in *Drosophila* eggs and lateral line primordium migration in zebrafish (Montell, 2008; Friedl and Gilmour, 2009).

Angiogenesis is a multicellular phenomenon whereby new blood vessels emerge from an existing vascular network in developmental and (patho)physiological contexts. Current understanding of angiogenesis encompasses tip cell selection by lateral inhibition, elongation, branching, anastomosis, vessel stabilization and lumen formation (Holderfield and Hughes, 2008; De Smet et al., 2009). Endothelial cell (EC) signaling involving the vascular endothelial growth factor (VEGF)-receptor (VEGFR), angiopoietin-Tie2 and Ephrin-Eph pathways has been intensively elucidated its role in these events (Armulik et al., 2005; Holderfield and Hughes, 2008; Gaengel et al., 2009). In addition, the interaction between ECs and mural cells (MCs), including vascular smooth muscle cells and pericytes, has also been implicated in the maintenance of the angiogenic process for appropriate organization (Hellstrom et al., 2001; Lafleur et al., 2001; Armulik et al., 2005; Gaengel et al., 2009; Liu et al., 2009).

Department of Physiological Chemistry and Metabolism, Graduate School of Medicine, The University of Tokyo, 7-3-1, Hongo, Bunkyo-ku, Tokyo, 113-0033, Japan.

*These authors contributed equally to this work
†Author for correspondence (nkanako@bio.m.u-tokyo.ac.jp)

Accepted 22 August 2011

Despite the extensive past studies, how the spatiotemporal regulation of molecules affects morphogenetic cell movement and what type of collective cell movement is involved in angiogenesis remain elusive, largely owing to the lack of a stable methodology for visualizing and assessing EC movements during angiogenesis. It is only recently that research has begun to focus on and assess real-time EC behavior during these processes (Murakami et al., 2006; Perryn et al., 2008; Vitorino and Meyer, 2008). In order to clarify the relationship between individual cell movements and angiogenic morphology, and to dissect the underlying molecular and cellular mechanisms, we first established a system in which dynamic cell behavior is visualized using time-lapse microscopy and set out to identify patterns of cellular behavior in an angiogenesis model through computational data processing. Surprisingly, cell movements were far more dynamic and heterogeneous in movement than previously thought. In elongating branches, ECs moved changing their relative positional relationships to each other at the tip. This 'cell-mixing' phenomenon was also confirmed in developing murine retinal vessels in vivo.

We further established a computer-assisted quantitative analysis system with which we can assess molecular and cellular mechanisms underlying complex EC movements. After validation of this system by analyzing the angiogenic effect of VEGF, we applied it to determining the role of Notch-related signaling in angiogenesis.

Recently, roles of Delta-like 4 (Dll4)-Notch signaling in angiogenesis have been demonstrated by a series of reports (Ridgway et al., 2006; Hellstrom et al., 2007; Siekmann and Lawson, 2007; Suchting et al., 2007). Murine retina heterozygous for a null mutation of the *Dll4* gene showed excessive branching and this was recapitulated by administering a γ-secretase inhibitor,

DAPT. Zebrafish in which Dll4 signaling was abolished using morpholino knockdown had increased migratory cells in intersomitic vessels. Blockade of Dll4 resulted in deregulated angiogenesis with a rather paradoxical reduction in tumor size. All of these findings have been attributed to a signaling cascade in which Dll4, by acting through Notch1, regulates tip cell differentiation. However, reports focusing on how individual EC movements are integrated into vascular morphology remain scarce.

The present analysis revealed that EC-EC interplay via Dll4-Notch signaling counter-regulated not only VEGF-induced tip cell behavior but also directed migration of stalk cells. In addition, EC-MC interplay might positively regulate EC behaviors, implying a novel role for MCs in the early stage of angiogenesis.

These findings, along with our time-lapse quantitative analyses, provide new insights into EC movements during angiogenesis, and the imaging and analysis system that we established should prove to be a powerful tool for linking individual cellular behaviors, molecular events and morphogenetic collective cell movements.

MATERIALS AND METHODS

Animals

ICR mice were purchased from Charles River Laboratories Japan and used in all experiments except for those on mice carrying the *Ednrd*^{Egfp} (*EGFP*-knock-in) allele (Asai et al., 2010). All animal experiments were reviewed and approved by The University of Tokyo Animal Care and Use Committee and were performed in accordance with the institutional guidelines.

Antibodies

The following antibodies were used: rat anti-CD31 (BD Pharmingen); rabbit anti-Dll4 and rat anti-platelet-derived growth factor receptor β (PDGFRβ) (Biolegend); rabbit anti-GFP (MBL); rabbit anti-NG2 and rabbit anti-phospho-histone H3 (PH3) (Millipore); and rat anti-PDGFRβ for neutralization (a gift from Dr Shin-ichi Nishikawa, RIKEN, Kobe, Japan).

Aortic ring assay and time-lapse live imaging

The aortic ring assay was performed as previously described (Blacher et al., 2001). Aortic rings were embedded in type I collagen gel (Nitta Gelatin) on eight-well chambered coverglasses (Nunc) and were cultured in medium-199 containing 5% FCS, 10 μg/ml streptomycin, 100 units/ml penicillin and 50 ng/ml human recombinant VEGF (R&D) (complete medium).

Time-lapse live imaging was started on the 5th or 6th day of the assay. For EC tracking, we labeled cells with SYTO-16 or SYTO-61 (0.1 μg/ml, Molecular Probes). Dynamic cell behavior was analyzed using a confocal laser scanning microscope (FluoView FV10i Olympus). Time-lapse live images were taken at 8-10 μm intervals for the *z*-axis every 15 minutes over 36 hours (10× 0.4 NA air objective), and for some assays, at 3 μm intervals every 5-7 minutes over 5-12 hours (60× 1.2 NA water-immersion objective). Obtained images were processed with analysis software FLUOVIEW (Olympus).

For mosaic analysis, the aortic ring was infected with adenovirus carrying EGFP (1×10^5 p.f.u./ml) (a gift from Dr Hideyuki Sakoda, The University of Tokyo, Japan) before cultivation. If needed, cells were incubated with 5 μg/ml of BS-1 lectin to visualize ECs.

Chemical interventions

To examine the effect of VEGF on sprouting angiogenesis, culture media were replaced with medium-199 containing 5% FCS, 10 μg/ml streptomycin, 100 units/ml penicillin and the indicated dose of VEGF 3 hours prior to time-lapse imaging. To inhibit Dll4-Notch signaling, sprouts were pre-treated with 50 μg/ml anti-Dll4-Ab (Yamanda et al., 2009) or 3 μM N-[N-(3,5-difluorophenacetyl-L-alanyl)]-S-phenylglycine t-butyl ester (DAPT, Sigma), a γ-secretase inhibitor, 24 hours prior to time-lapse live imaging. For morphological analysis, anti-Dll4-Ab or DAPT was added throughout the assay. To inhibit the PDGFRβ signal, cells were treated with anti-PDGFRβ-Ab (10 μg/ml) in complete medium throughout the assay (Uemura et al., 2002).

In vivo EC-tracking analysis

To label ECs of the retinal vasculature intravascularly, 3-5 μg of fluorescent-conjugated BS-1 lectin (Sigma) was injected into the cardiac chamber of neonatal mice beginning on postnatal day 1 using glass capillary pipettes. Retinas were obtained at the indicated time after the injection.

In silico analysis

Cell tracking, data extraction and data analysis were carried out using ImageJ, MTrackJ and MATLAB.

Cell tracking

Nuclei of each EC were manually selected, and whenever two or more nuclei overlapped, general rules were applied to define the next points of the current track: (1) when there is obvious flow of cells in one direction, a cell is likely to move on that axis either anterograde or retrograde, albeit with some deviation; (2) in the setting of (1) and when there are two or more candidate axes, cells are prone to move on their previous axis and in their prior direction; (3) in the setting of (2), when there are more than two candidate positions for the next slice, either the nearest possible and/or the one most likely regarding the previous velocity is chosen; and (4) normally, cells avoid bumping into each other by fine-tuning their velocities and directions.

Definitions

The term 'tip cells' refers to 'cells at the tip of a certain time point'. The other, non-tip cells, were termed 'stalk cells'. A branch was defined as a multicellular protrusion with more than two ECs. A 'junction' was defined as a point of divergence, juncture or intersection of several vessels, and a 'stalk' was the region distal to a junction. The area of analysis was defined by setting four coordinates that surround all nuclei in a stalk or a junction. The latter was set to exclude as the cells of distal stalks as much as possible.

The axis and direction of elongation (elongation vector, $\boldsymbol{E}$) was defined as $\boldsymbol{E}=\boldsymbol{r}(end)-\boldsymbol{r}(0)$, where $\boldsymbol{r}(t)$ stood for the coordinates of the tip at $time=t$ ('end' stands for the last observed time point). When a branch sprouted out after the start, $t=0$ meant the start of elongation and thus of the sprouting event. To this end, the tip was tracked independently. The coordinates of each cell were calculated by orthogonal projection to the axis of elongation. Therefore, $e(i,t)=dot[\boldsymbol{E},(\boldsymbol{r}(i,t)-e0)]/|\boldsymbol{E}|$, where $e(i,t)$ stood for the one-dimensional coordinates of a cell with an $ID=i$ at $time=t$ obtained by orthogonal projection. $\boldsymbol{r}(i,t)$ was the original coordinates of i-th cell at $time=t$. 0 on this axis meant the initial coordinates of the tip ($e0$) projected to the elongation vector, and $dot[\boldsymbol{A},\boldsymbol{B}]$ was the internal product of vectors $\boldsymbol{A}$ and $\boldsymbol{B}$. The coordinates of a cell with an $ID=i$ at $time=t$ were represented as vector $\boldsymbol{r}(i,t)$. $|\boldsymbol{A}|$ stood for the absolute value of vector $\boldsymbol{A}$; thus, $|\boldsymbol{A}|=sqrt(dot[\boldsymbol{A},\boldsymbol{A}])$, where $sqrt(\boldsymbol{a})$ was the square root of $\boldsymbol{a}$. The coordinates were plotted against time.

The point at which a cell was overtaken was visually determined as when the centroid of the pre-existing tip cell fell behind that of the cell coming from behind for at least two frames. For tip cell parameters, 'elongation drive' (net elongation of a branch)/(number of tip cells during the total observed time) and 'tip duration' (overall time)/(number of tip cells during the total observed time) were introduced. For parameters at stalks and junctions, the 'coordination' index was set. The angle $[\theta(i,t)]$ between the direction of elongation or the bisector (elongation direction, $\boldsymbol{D}$) and the moving direction of a cell [velocity vector, $\boldsymbol{v}(i,t)$] was calculated and plotted against time. $\boldsymbol{D}$ was set so as to face the direction of net cell flow, parallel to the axis of the distal stalk, or the bisector of distal stalks if there were two outflows, at junctions. The angle was calculated by the equation, $\theta=Arccos(dot[\boldsymbol{D},\boldsymbol{v}]/|\boldsymbol{D}||\boldsymbol{v}|)$, where θ ranges from 0 to π and $\boldsymbol{v}=\boldsymbol{v}(i,t)=\boldsymbol{r}(i,t+15)-\boldsymbol{r}(i,t)$. Thus, in coordinated junctions, θs were expected to be narrowly distributed around the mean. Quantification was performed by pooling the time series and taking the standard deviation (Std) for anterograde ($\theta<\pi/2$) and retrograde ($\theta>\pi/2$) separately. The 'orientation' index was defined as (net displacement of the cell)/(total length of the track of a cell). Net displacement of a cell [$\boldsymbol{R}(i)$] was calculated by $\boldsymbol{R}(i)=|\boldsymbol{r}(i,end)-\boldsymbol{r}(i,start)|$, where '*start*' and '*end*' referred to the time points at which the cell enters ('*start*') and moves out of ('*end*') the analyzed area, and the total

length of the track of a cell [$L(i)$] was calculated by $L(i)=\Sigma|v(i,t)|$, where sigma (Σ) was the summation for time ($t=start$ to $t=end$). A value near 1 means the cell has moved straight and with no change in direction in the analyzed area. Percentages of ECs moving forwards (anterograde, $\theta<\pi/2$), backwards (retrograde, $\theta>\pi/2$) or remaining (still, $v=0$) were also calculated as the ratio to the total number of cells observed in a particular stalk area throughout the period from $t=0$ to $t=end$ ('Directional motility'). ECs that moved fewer than 0.5 pixels were counted as stopped. Finally, mean absolute velocity ($<v(i)>$) at a specific area of analysis was calculated as $<v(i)>=\Sigma|v(i,t)|/\Delta t$, where Δt stood for the time interval between the start and the end.

Whole-mount staining and imaging

For murine aortic assays, whole-mount staining was performed as described previously (Yamashita et al., 2000). If needed, nuclei were counterstained with TOPRO3 (Invitrogen). For live cell imaging, SYTO-dye-stained cells were immunostained with fluorescent-conjugated anti-CD31- and PDGFRβ-Abs for 30 minutes prior to imaging. In the murine retina, whole-mount immunostaining was performed as previously described (Uemura et al., 2002). Fluorescent signals were visualized with a computer-assisted confocal microscope (Nikon D-ECLIPSE C1). Photomicrographs were obtained at 1-10 μm intervals as necessary and reconstituted using EZ-C1 software (Nikon). Signals were also visualized by an enzymatic reaction with 3,3′-diaminobenzidine (Dojin) chromogen, and photographs were obtained with a phase-contrast microscope (Nikon TE300, Tokyo, Japan).

Proliferation analysis

Mitotic events were detected on movies (see Fig. S2A in the supplementary material). The percentage was calculated by dividing the number of ECs undergoing mitosis at specified places by the total number of ECs appearing in an observed movie. Mean observed time per cell was also calculated. In addition, angiogenic sprouts were immunostained with PH3, a marker of mitosis (Hendzel et al., 1997; Dai et al., 2005), at day 7. The number of $PH3^+$ ECs was counted in randomly selected areas (including the sprout from the bottom to the tip), and the rate of $PH3^+$ ECs to total ECs per ring was calculated. Furthermore, observed areas were divided into two specified areas ('distal 400', 400 μm area proximal to the tip; 'proximal', the area more proximal than the 'distal 400'). Similar analyses were performed for murine retinal angiogenesis.

Morphology analysis

Z-stack images of $CD31^+$ endothelial sprouts were obtained using a confocal microscope as described above. After optimization on Photoshop, endothelial sheet-forming areas and parts of the explanted ring were manually eliminated. The total length of angiogenic sprouts was then measured on the converted binary images using the NeuronJ plug-in for ImageJ ('total length'). The total number of branching points was manually counted ('total branch points') and the 'relative branch point' was defined as ('total branch points')/('total length'). The 'mean width' was calculated by dividing total area of the sprouts by 'total length'.

Flow cytometry

After the explanted rings had been manually extracted from type I collagen gels, the gels were incubated in medium-199 containing 1 mg/ml collagenase (Sigma) at 37°C for 30 minutes, followed by incubation with 0.05% trypsin-EDTA (Sigma). The cells were immunostained with an anti-CD31-Ab conjugated with PE on ice. Analyses were performed on a FACS VantageSE flow-cytometer (BD Biosciences), and data were analyzed with CellQuest software (BD Biosciences). In the assay, nonviable cells stained with propidium iodide (Sigma) were excluded by electronic gating.

RT-PCR

Cells were harvested as described above. Extracted total RNA was reverse-transcribed using a conventional method. For semi-quantitative RT-PCR, the resultant cDNAs were amplified with *Taq* polymerase (Takara) in a thermocycler. The primer pairs used were as follows: for murine Hes-1, 5′-TCATGGAGAAGAGGCGAAGG/GTATTTCCCCAACACGCTCG-3′; for murine Hey2, 5′- CCGAGAGTGCTTGACAGAAGTG/TGTGGGGA-GATGGTGGAAA-3′; for murine CD31, 5′-AGGACAGACCCTTCCA-CCAA/AATGACAACCACCGCAATGA-3′; and for murine GAPDH, 5′-GGTGTGAACCACGAGAAATAT/AGATCCACGACGGACACATT-3′. Thermal cycling was performed for 18-30 cycles to maintain PCR conditions within the linear range of amplification before reaching saturation. Each cycle consisted of 30 seconds of denaturation at 94°C, 30 seconds of annealing at 58°C and 1 minute of extension at 70°C.

Statistical analysis

All data were compared between groups using the Mann-Whitney test and Kruskal-Wallis test accompanied by multi-comparison analysis where necessary. Pearson correlations were used to evaluate the relations between vessel elongation and other parameters. The relationships between vessel elongation and other parameters were studied using a linear regression analysis, which was performed separately for models involving single or multiple independent variables. The variance inflation factor was also estimated for all independent parameters in order to evaluate co-linearity. $P<0.05$ was considered significant. Data in bar graphs were represented as means±s.e.m.

RESULTS

Fluorescent imaging of ECs during in vitro angiogenesis

To characterize the behavior of vascular ECs during angiogenic morphogenesis, we visualized the dynamics of cell movement during in vitro angiogenic processes in a murine aortic ring assay (Blacher et al., 2001), using time-lapse microscopy. In this assay, various modules of the angiogenic processes such as endothelial sheet formation, sprouting, circumferential growth, branching and the resultant formation of a characteristic dendritic architecture were observed under VEGF stimulation (Fig. 1A). The sprouts of $CD31^+$ ECs were covered with $NG2^+$, $PDGFR\beta^+$ MCs (Ozerdem et al., 2001; Armulik et al., 2005), and also characterized by endothelin receptor type A (*Ednra*)-EGFP knock-in gene expression (Asai et al., 2010) (Fig. 1B-D).

To identify and track individual ECs in the multicellular structure, the nuclei of living cells were labeled with a cell-permeable fluorescent SYTO dye, by which we succeeded in selectively labeling EC during angiogenic morphogenesis (Fig. 1E-G; see Fig. S1 in the supplementary material; see also Movies 1 and 2 in the supplementary material). Although nuclear staining was not specific for ECs, we found that ECs could be distinguished from MCs covering endothelial sprouts by their signal intensity: whereas ECs showed intense staining with SYTO dyes, morphologically distinguishable or $Ednra\text{-}EGFP^+$ MCs were minimally stained (Fig. 1F; see Fig. S1C and Movie 2 in the supplementary material). In addition, this was supported by the results of live cell staining and imaging, which demonstrated that cells intensely stained with SYTO dyes were positive for CD31, whereas faintly stained cells were negative for CD31 or positive for PDGFRβ (Fig. 1G; see Fig. S1A,B in the supplementary material). The difference in SYTO dye stainability was further confirmed by flow-cytometric analysis (see Fig. S1D in the supplementary material). Thus, differences in nuclear staining as well as in morphology were used to visually distinguishing ECs from MCs.

Time-lapse live imaging reveals complexity of EC behavior during in vitro angiogenesis

In the aortic ring assay, elongation and bifurcation of an existing branch were evident. However, cellular behaviors underlying these events were far more complex and heterogeneous than expected (Fig. 2A; see Movie 1 in the supplementary material).

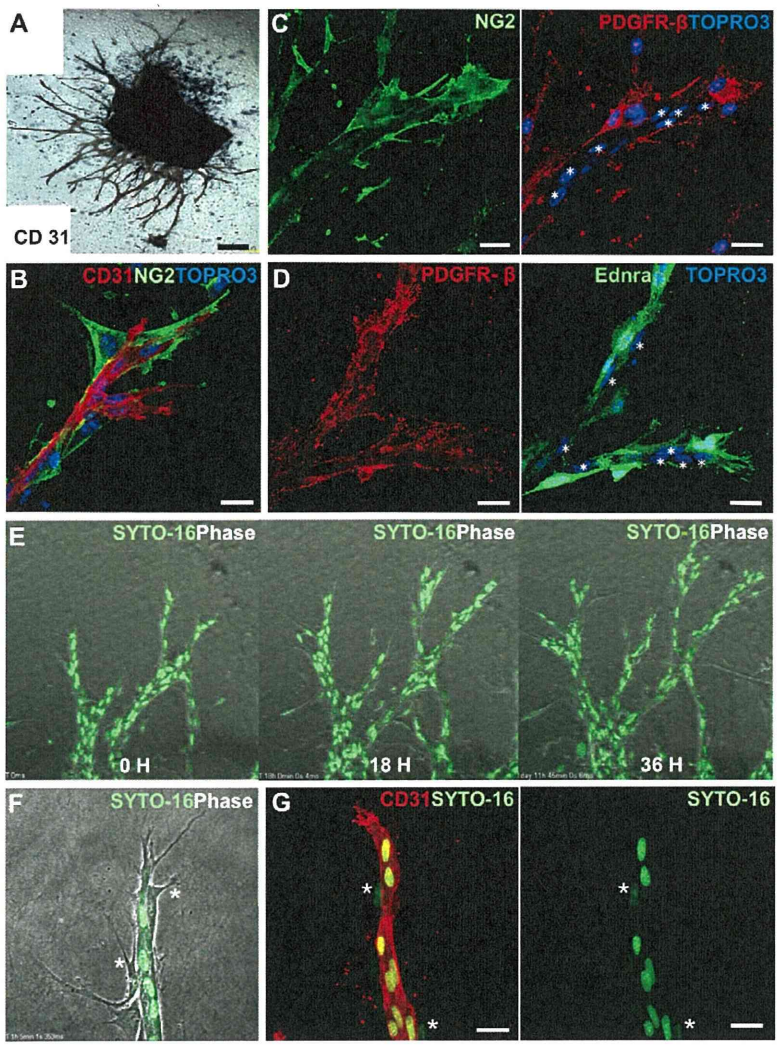

Fig. 1. Establishment of EC-tracking system in murine aortic ring assay. (**A**) CD31$^+$ EC sprouts protruding from an aortic ring explant. (**B-D**) CD31$^+$ EC sprouts are covered with MCs positive for NG2 (B), PDGFRβ (C) and Ednra-EGFP (D). Asterisks indicate nuclei of ECs. (**E**,**F**) Merged images of confocal and phase-contrast views. Nuclei were stained with SYTO dye. (E) Time-lapse images (see also Movie 1 in the supplementary material). (F) Nuclei in MCs (asterisk) were only faintly stained by SYTO dyes when compared with those in ECs. (**G**) Immunostaining confirmed that strongly SYTO dye-stained cells were CD31$^+$ ECs. Asterisks indicate CD31$^-$ MCs. Scale bars: 250 μm in A; 25 μm in B-D,G.

Individual ECs moved forwards and backwards along the path of the elongation in stalks and junctions, changing their velocity. At the tip region, fast cells overtaking other ECs become the new tip, indicating replacement of tip cells ('overtaking of the tip cell'). As a result, relative positional relationship of ECs was dynamically changed ('cell-mixing'). This 'cell-mixing' phenomenon was clearly shown by labeling cells segmentally with different colors (Fig. 2A; see Movie 1 in the supplementary material). Although the elongating process was dynamic, the frequency of cell division was very low at around 5% of total ECs in the observed time (mean observed time per cell was 22.4 hours), even in the presence of VEGF (see Table S1 in the supplementary material). Consistently, we observed that the number of PH3$^+$ ECs was quite low (0.8% of total observed ECs), with lower frequency in the proximal region (see Fig. S2B,C in the supplementary material). Observations were similar for murine retinal angiogenesis at P1 and P3 (see Fig. S2B,C in the supplementary material), also consistent with a previous report (del Toro et al., 2010). These results suggest that elongation and branching in the observed area are attributable mainly to EC migration rather than to proliferation.

Dynamics of cell movement during branch elongation

To further elucidate cell behavior in an elongating branch, we developed a trajectory analysis, which enabled us to evaluate visually and quantitatively single- and multi-cellular movements, as well as to compare the dynamics of cell movement between branches elongating in different directions (Fig. 2B; see Fig. S3 in the supplementary material). Trajectory analysis revealed that branch elongation was a repeated event in which an EC at the stalk overtook the tip cell to become the new tip (Fig. 2B, part a). The new tip cell became less motile after this overtaking (arrow), followed by being overtaken by another cell (arrowhead). Thus, branch elongation appeared to be promoted by repetitive overtaking (a dark-blue trajectory in Fig. 2B, part a). In some cases, a tip cell was overtaken by another EC (arrow) and then retreated to become a tip cell again (arrowhead) (purple trajectory in Fig. 2B, part b). Furthermore, overtaking (arrow) by a fast-moving EC from far behind (fast EC, a pink trajectory in Fig. 2B, part c) seemed to contribute to effective branch elongation. In a poorly elongating branch, overtaking by a fast EC was rare (arrowhead in Fig. 2B, part c). However, overtaking by a fast EC alone was not sufficient

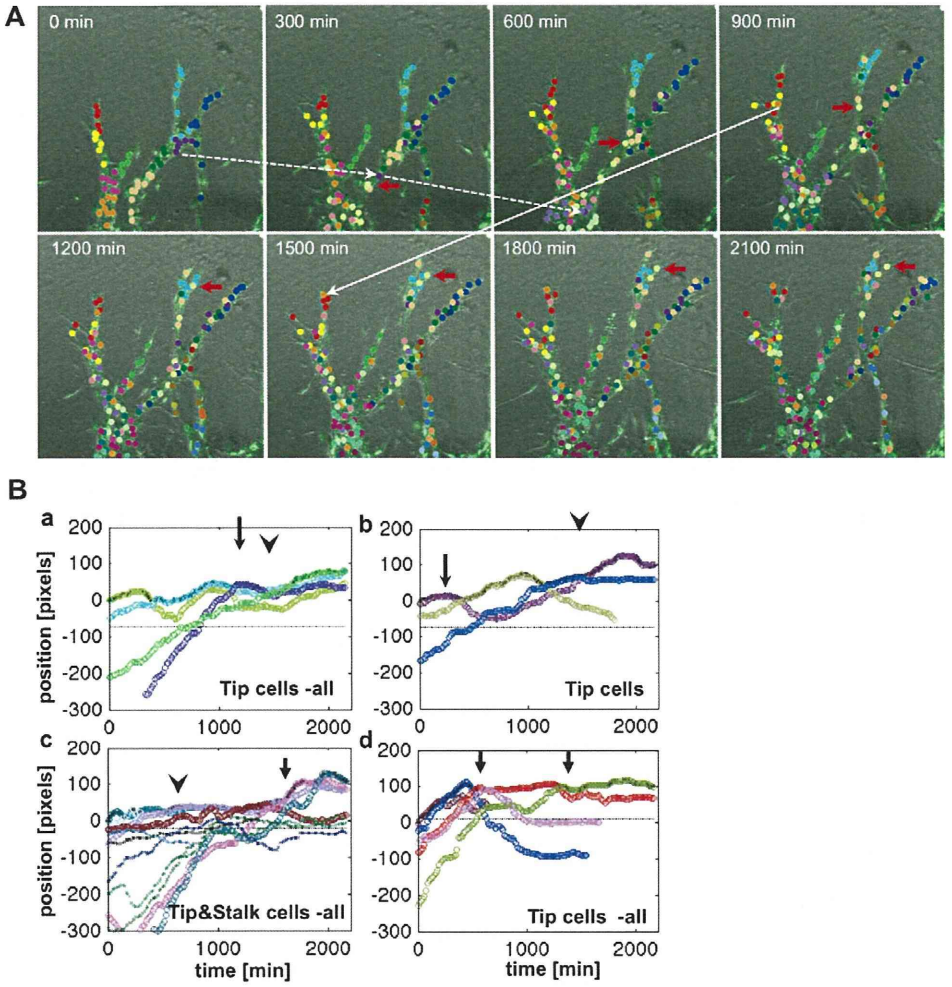

Fig. 2. Time-lapse live imaging and computational analysis reveals complexity of EC behaviors during in vitro angiogenesis. (**A**) SYTO dye-staining and time-lapse imaging were performed in the aortic ring assay. *Z*-stack confocal images were overlaid on the phase-contrast images. Nuclei were tracked using MTrackJ and the centroids of these nuclei are pseudocolored clusterwise. Initial clusterwise labeling becomes increasingly obscure over time ('cell-mixing'). Yet ECs are seen to move faster than others and become the new tip (white and red arrows). Some other ECs are seen to move in the direction opposite elongation (broken arrow) (see also Movie 1 in the supplementary material). (**B**) Trajectory analysis. Representative patterns of EC movements during branch elongation are shown. Cells that became tip cells at some point are represented by thick lines; individual cells are presented in different colors (see also Fig. S3 in the supplementary material). (a) Repeated overtaking of the tip cell during branch elongation. (b) Repetitive overtaking of the tip cell by an EC. (c,d) Overtaking by a fast-moving EC resulting in effective branch elongation (c) or not (d).

for elongation because some branches with overtaking by a fast EC did not show effective elongation (arrows in Fig. 2B, part d), suggesting that other conditions in which overtaking by a fast EC leads to effective elongation are also necessary.

Mosaic analysis confirms 'cell-mixing' phenomenon during in vitro angiogenesis

To confirm whether the identified phenomena such as 'cell-mixing' based on nuclear tracking occur on a whole-cell basis, we performed a mosaic analysis by visualizing the cytoplasm with EGFP. In this analysis, ECs could be identified by differences in the intensity of SYTO dye staining and, in some cases, staining for BS-1 lectin (Fig. 3). Mosaic analysis revealed that high EGFP-labeled EC (red arrows in Fig. 3A) appeared to 'slip' forward on the surface of a tip cell, overtaking and then being replaced by a follower EC without the EGFP signal (yellow arrows), which confirmed overtaking of the tip cell at a cellular level (see Movie 3 in the supplementary material). Mosaic analysis further showed that highly motile ECs displayed unidirectional forward-rear cell polarity, depending on the direction of movement, whereas minimally motile ECs were spindle-shaped without cell polarity (Fig. 3A-D; see Movies 3 and 4 in the supplementary material), and that the polarity of individual ECs was dynamically changed in conjunction with the motility (Fig. 3E; see Movie 5 in the supplementary material). These results provide a cellular basis for the phenomenon of angiogenic sprouting with 'cell-mixing'.

Identification of 'cell-mixing' phenomenon during murine retinal angiogenesis in vivo

Next, we verified whether the 'cell-mixing' phenomenon occurs in vivo. We labeled ECs by intravascular injection of a BS-1 lectin at postnatal day 1.0 and tracked them during mouse retinal

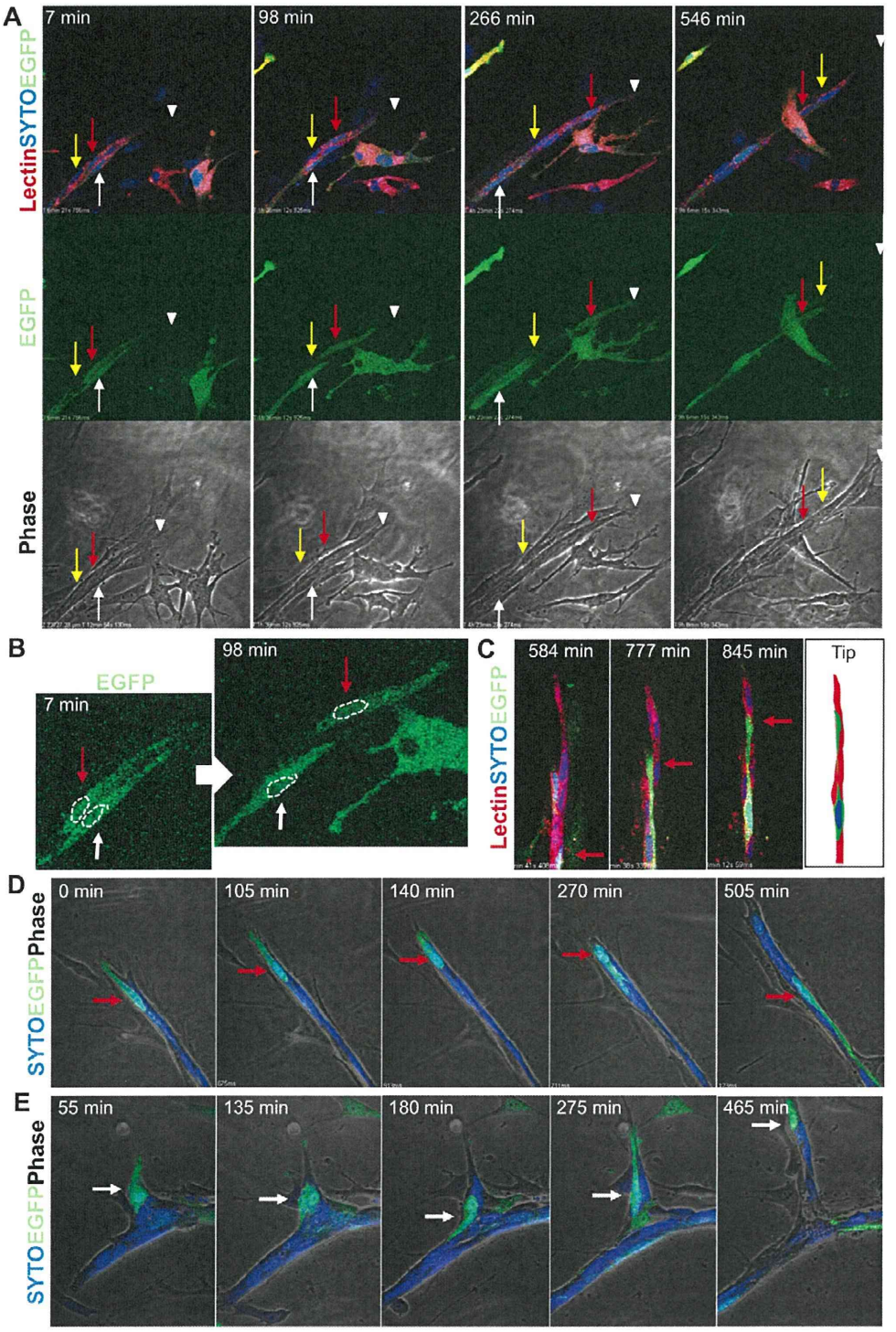

Fig. 3. Mosaic analysis reveals 'cell-mixing' phenomenon on whole-cell basis. In the aortic ring assay, in which cells were infected with a low titer of adenovirus carrying EGFP, time-lapse imaging was performed. ECs were identified by stainability with SYTO dye and/or BS-1 lectin. (**A**) Representative time-lapse images showing 'overtaking of the tip cell' (red and yellow arrows). White arrowheads indicate the tip of the endothelial sprout. White arrows indicate minimally motile ECs. (**B**) Higher magnification images of A, showing highly motile (red arrow) and minimally motile (white arrows) ECs. Broken circles indicate nuclei (see Movie 3 in the supplementary material). (**C**) Another example of a highly motile EC (red arrow). (**D**) Cell polarity changed dynamically depending on the direction of movement (red arrow) (see Movie 4 in the supplementary material). (**E**) An EC (white arrow), which lost cell polarity just before being overtaken by a follower (135 minutes), generated cell polarity again at 275 minutes and again started moving to the tip (see Movie 5 in the supplementary material).

angiogenesis (Fig. 4A). At this stage, sprouting angiogenesis takes place on the retinal surface (Fig. 4B), and tip and distal stalk cells do not form a lumen (Gerhardt et al., 2003). Consistent with previous findings, the proximal (lumen-forming) regions of $CD31^+$ endothelial sprouts were uniformly and reproducibly labeled by lectin shortly after its injection, whereas the distal regions (including the tip) were not (Fig. 4C). As expected, 6 hours after the injection, lectin-positive and -negative cells were colocalized at the distal regions in a mixed pattern. Typically, a $CD31^+$ EC at the tip and some follower ECs were lectin positive in the distal regions (Fig. 4C; see Fig. S4A in the supplementary material), indicating that the ECs around the tip came from the proximal regions forming the lumen. Similar mosaic patterns were also observed at the distal and proximal positions of sprouts 12 hours after the lectin injection (see Fig. S4B in the supplementary material). Collectively, these results strongly suggest that the 'cell-mixing' phenomenon occurs during in vivo retinal angiogenesis.

Quantification of EC behaviors driving angiogenic morphogenesis

In order to unravel the cell-based mechanism that drive angiogenic morphogenesis and dissect the underlying molecular networks, we first set out parameters to quantify different angiogenic modules. VEGF also promoted angiogenesis in our setting (Fig. 5A; see Movie 6 in the supplementary material). One of the pro-angiogenic effects of VEGF is to elongate vessel branch, characterized herein by an increase in the index 'vessel elongation' (Fig. 5C), owing to the increased number of ECs in the branch (Fig. 5D). The tip of an elongating branch overtaking ECs was identified (Fig. 5B). Because overtaking of tip cells occurred regardless of the presence or absence of VEGF, we established 'elongation drive' (displacement per tip cell) and 'tip duration' (the time spent as a tip cell) parameters to quantify events at the tip further (Fig. 5B). Interestingly, VEGF-induced vessel elongation was closely associated only with greater elongation drive (Fig. 5C). Overtaking of tip cells occurred similarly at interval ranging from ~350 to ~900 minutes, whether or not VEGF was present. These results indicate that VEGF positively affects tip cell behaviors following overtaking without changing the frequency of overtaking.

We also set the following parameters to evaluate the complex cell movements at junctions and stalks: mean migratory velocity, coordination (whether or not ECs moved in the same direction (coordinated)), orientation (whether or not a single cell moved straightly), and directional motility (whether or not ECs migrated toward the direction of branch elongation) (Fig. 5E). In the

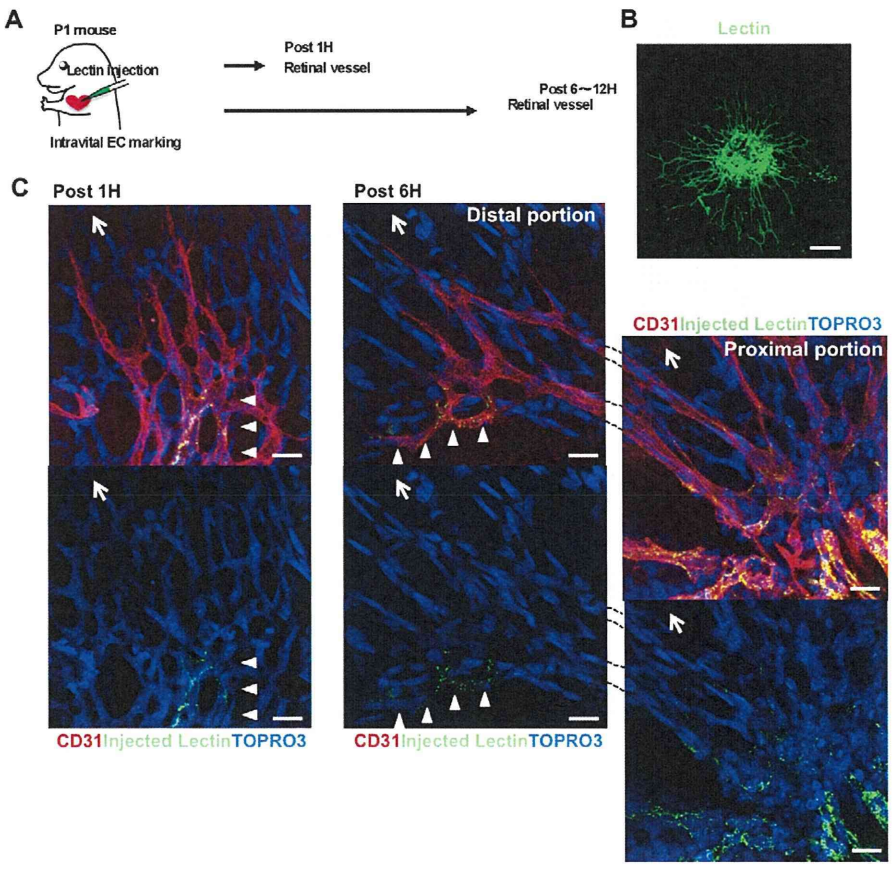

Fig. 4. Identification of 'cell-mixing' phenomenon during murine retinal angiogenesis in vivo. (**A**) BS-1 lectin was injected into the cardiac chamber at postnatal day 1 (P1) to label ECs transvacularly. Labeled ECs were observed in retinal angiogenesis 6 hours after the injection. (**B**) Whole-mount staining of the retinal vasculature with BS-1 lectin at P1. (**C**) *Z*-stack confocal images. Nuclei were stained with TOPRO3. The proximal regions of $CD31^+$ endothelial sprouts were uniformly labeled by injected lectin (arrowheads), whereas the distal regions (including the tip) were not at 1 hour after the injection. Six hours after the injection, lectin-labeled ECs (arrowheads) were also observed in some distal regions of the sprouts. Arrows show the direction of vessel elongation. Scale bars: 100 μm in B; 25 μm in C. See Fig. S4 in the supplementary material.

DEVELOPMENT